Supporting Information

Solution-Processed Sensing Textiles with Adjustable Sensitivity and Linear Detection Range Enabled by Twisting Structure

Zengyu Hui,[†Δ] *Ruyi Chen,*[†Δ] *Jin Chang,*[†Δ] *Yujiao Gong,*[†] *Xianwang Zhang,*[§] *Hai Xu,*[†] *Yue Sun,*[†] *Yue Zhao,*[†] *Lumin Wang,*[†] *Ruicong Zhou,*[†] *Feng Ju,*[§] *Qiang Chen,*[‖] *Jinyuan Zhou,*[⊥] *Jianing An,*[¶] *Gengzhi Sun,**[†‡] *and Wei Huang*[†‡]

[†]Institute of Advanced Materials (IAM), Nanjing Tech University (NanjingTech), Nanjing 211816, P. R. China

[‡]Institute of Flexible Electronics (IFE), Northwestern Polytechnical University (NPU), Xi'an 710072, P. R. China

[§]School of Mechanical and Electrical Engineering, Nanjing University of Aeronautics and Astronautics, Nanjing 210016, P. R. China

[‖]School of Materials Science and Engineering, Henan Polytechnic University, Jiaozuo 454003, P. R. China

[⊥]School of Physical Science and Technology, Lanzhou University, Lanzhou 730000, P. R. China

[¶]School of Mechanical and Aerospace Engineering, Nanyang Technological University, 50 Nanyang Avenue, 639798, Singapore

[*]Corresponding author. E-mail address: iamgzsun@njtech.edu.cn

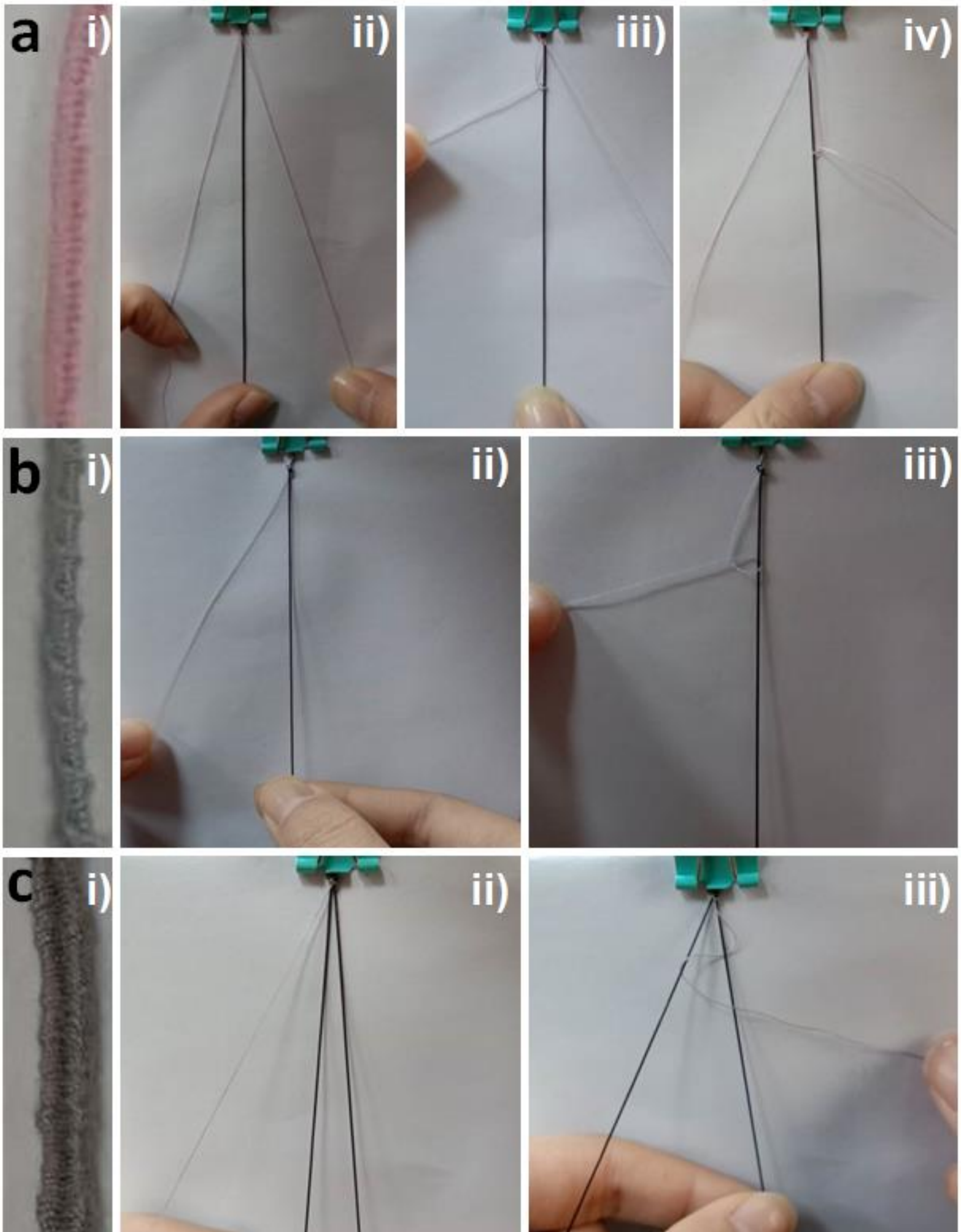

Figure S1. Twisting procedures for three predesigned models: a) Model 1, b) Model 2, and c) Model 3.

Figure S2. Photograph of as-prepared PPy without PVA.

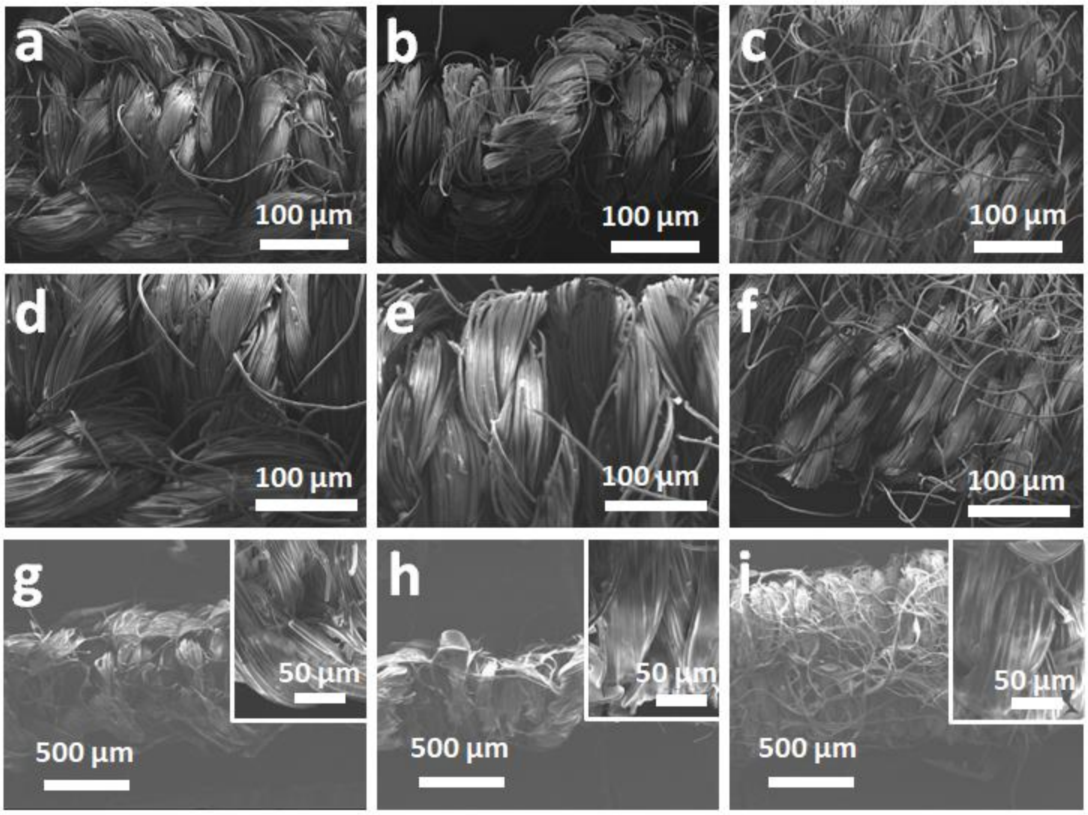

Figure S3. SEM images of the textiles before and after dip-coating: a-c) SEM images of as-twisted textiles of M1, M2, M3, respectively; d-f) high-magnification SEM images of original textiles of M1, M2, M3; g-i) SEM images of M1, M2, M3 dip-coated by conductive ink. Insets correspond to high-magnification SEM images of PPT-M1, PPT-M2 and PPT-M3.

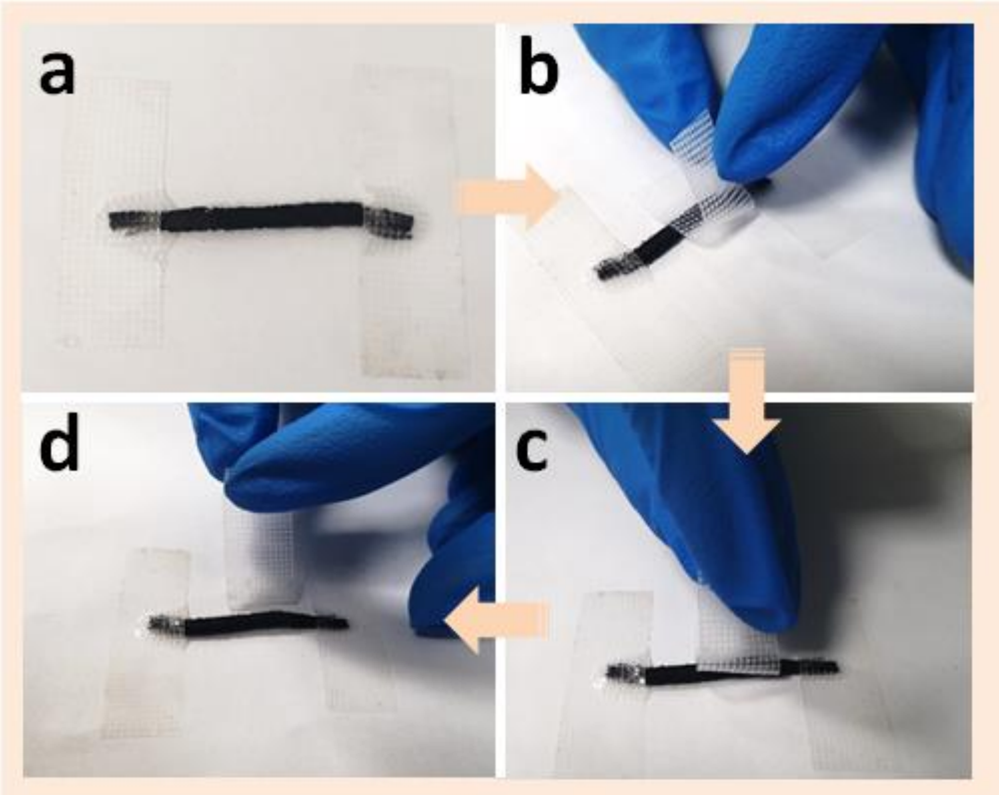

Figure S4. a-d) Demonstration of good adhesion between conductive sheath and core yarn by attaching onto and peeling off a adhesive tape.

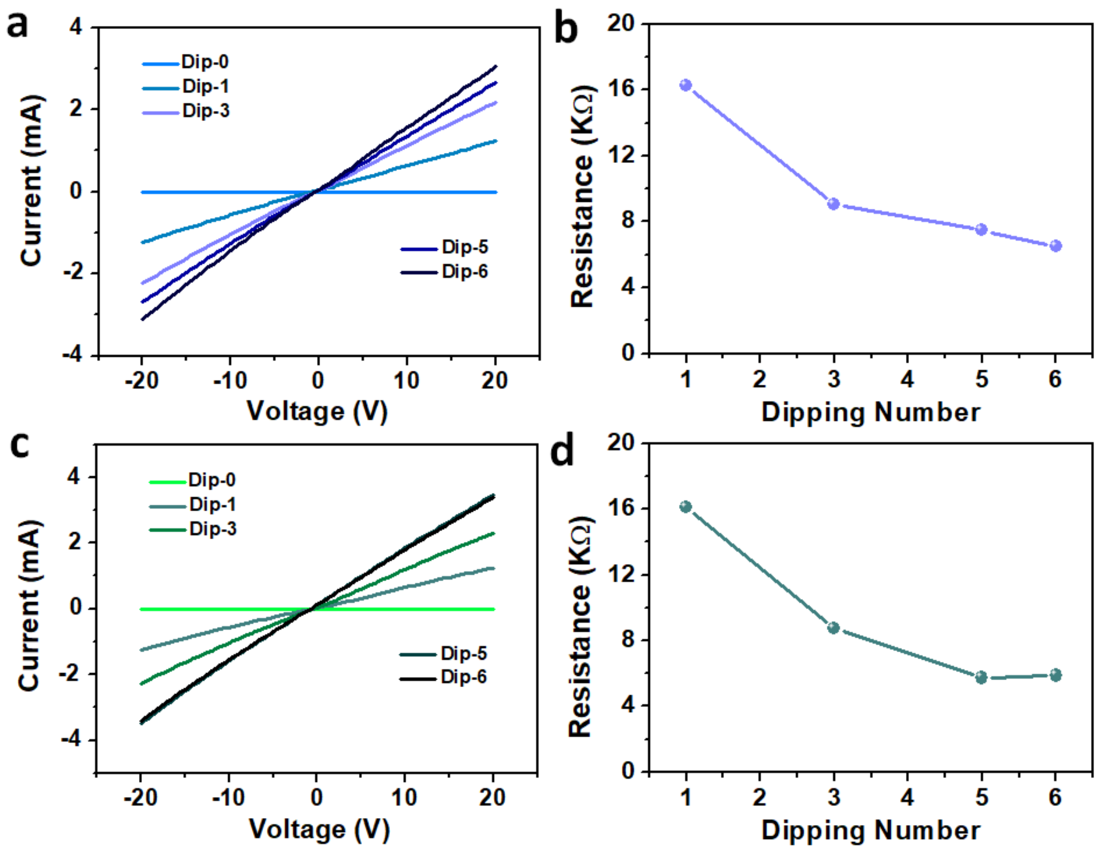

Figure S5. a) Current-voltage curve of PPTS-M1 with varying dip-coating times (one to six). b) Resistance of PPTS-M1 with varying dip-coating times. c) Current-Voltage curve of PPTS-M2 with varying dip-coating times (one to six). d) Resistance of PPTS-M2 with varying dip-coating times.

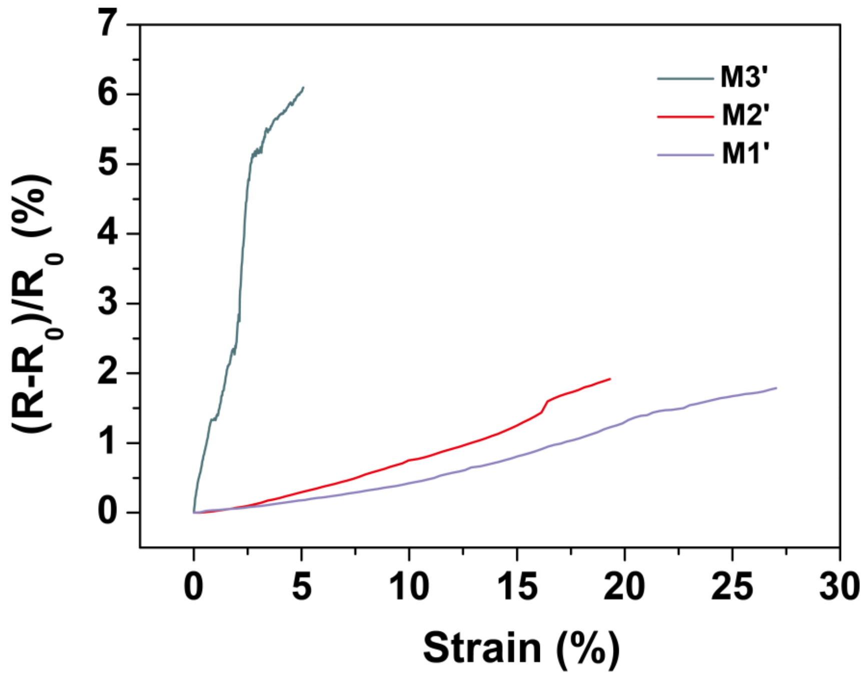

Figure S6. Resistance variation of three models without central elastomer during tension.

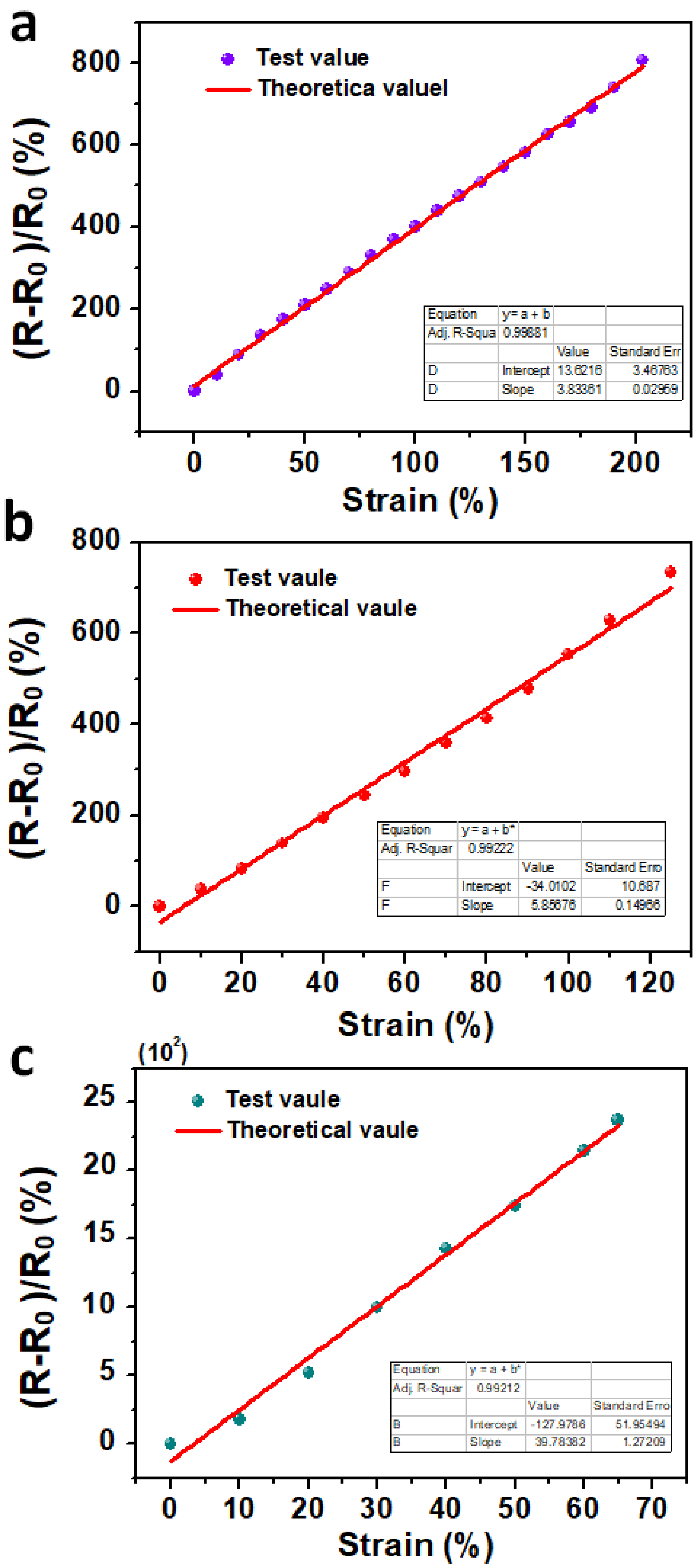

Figure S7. a-c) Linearity fit of resistance change for PPTS-M1, PPTS-M2 and PPTS-M3 during tension, respectively.

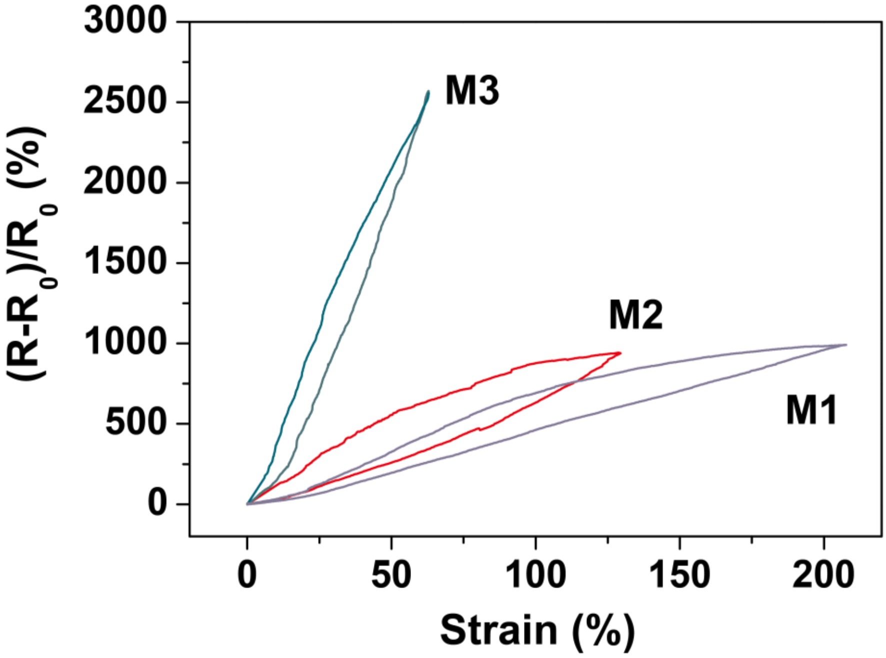

Figure S8. The hysteresis behavior of PPTS-M1, PPTS-M2 and PPTS-M3.

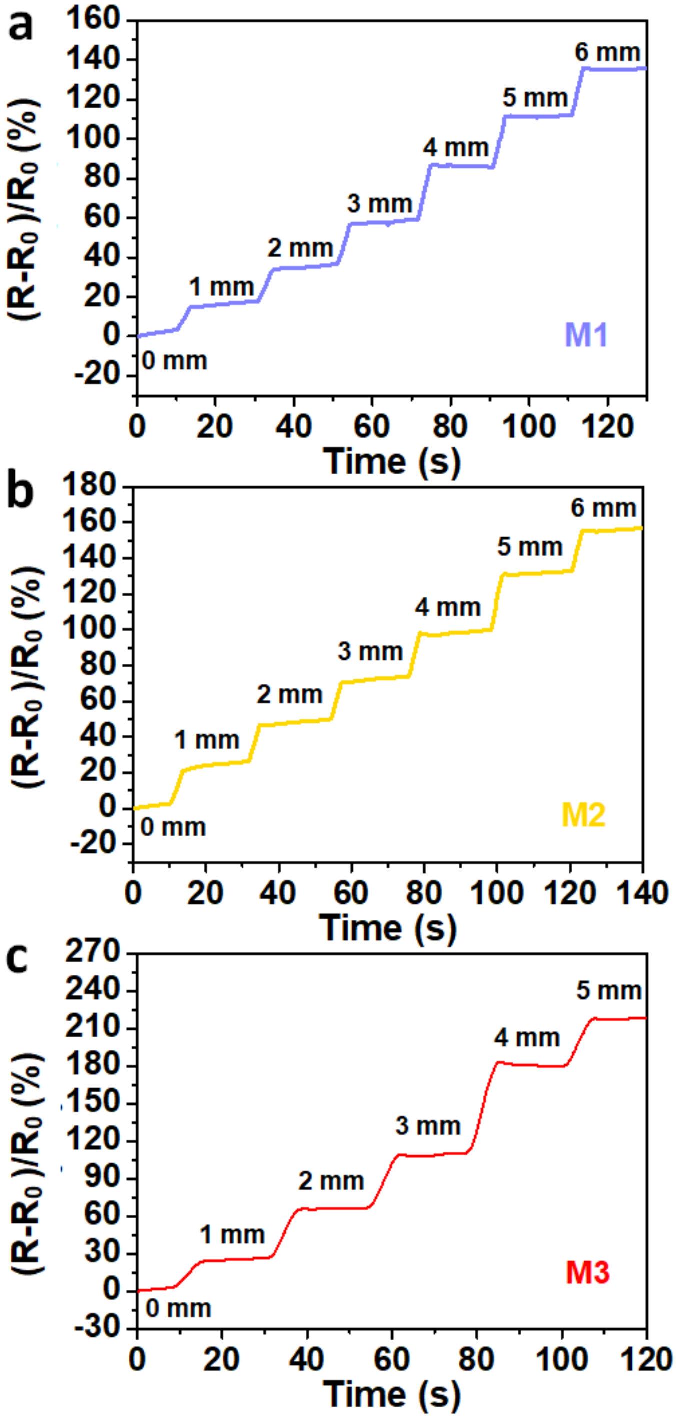

Figure S9. a-c) Relative resistance change of PPTS-M1, PPTS-M2 and PPTS-M3 at different strains.

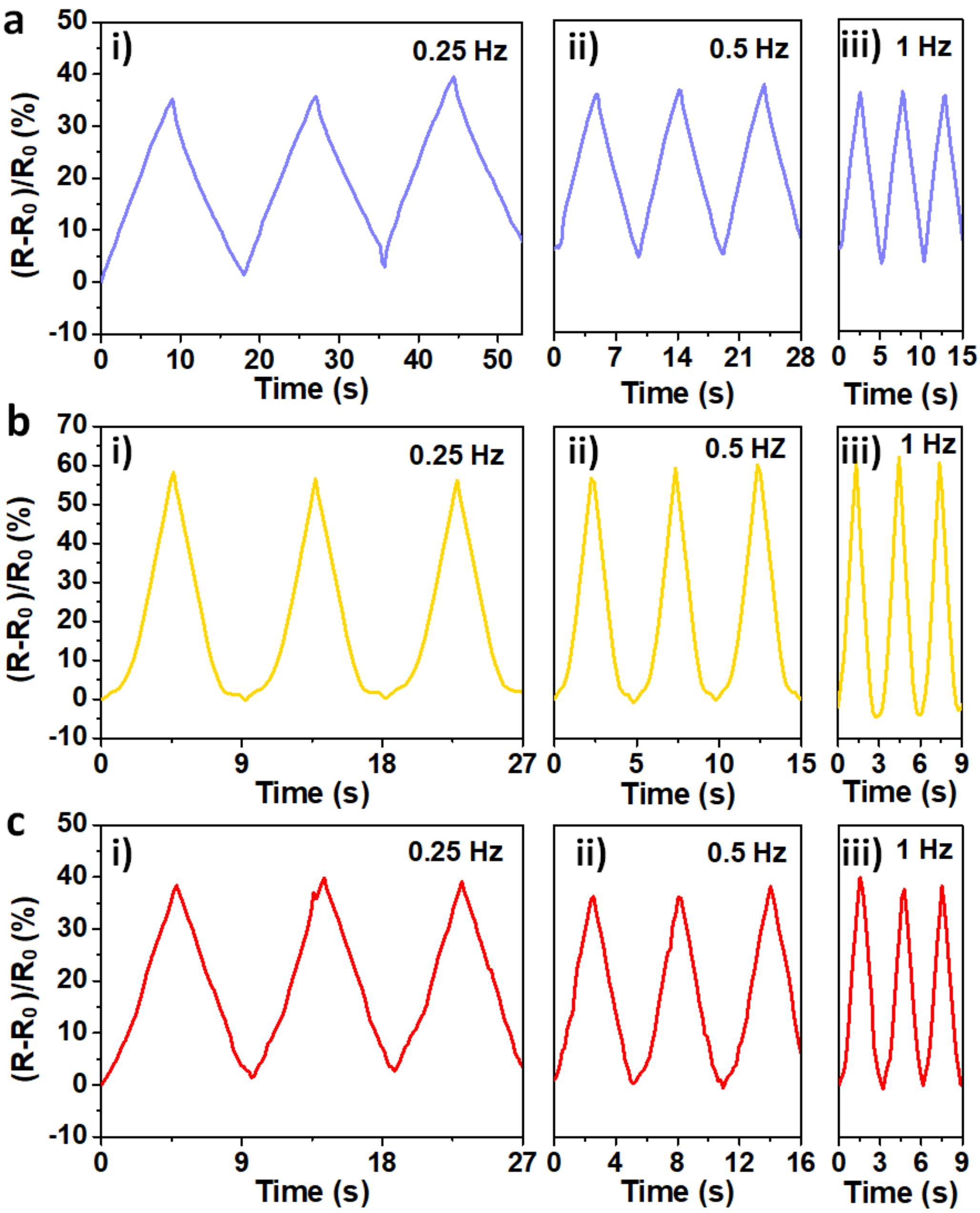

Figure S10. a-c) Relative resistance variation under cyclic stretching/releasing at frequencies of 0.25, 0.5, and 1 Hz for PPTS-M1, PPTS-M2 and PPTS-M3, respectively.

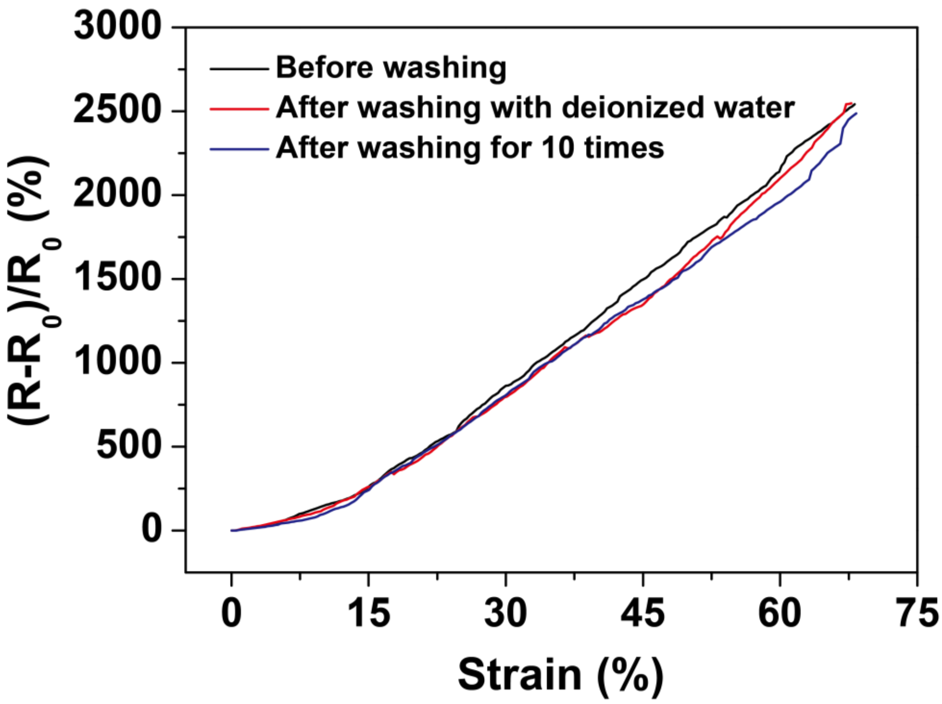

Figure S11. The performance of PPTS-3 before and after washing.

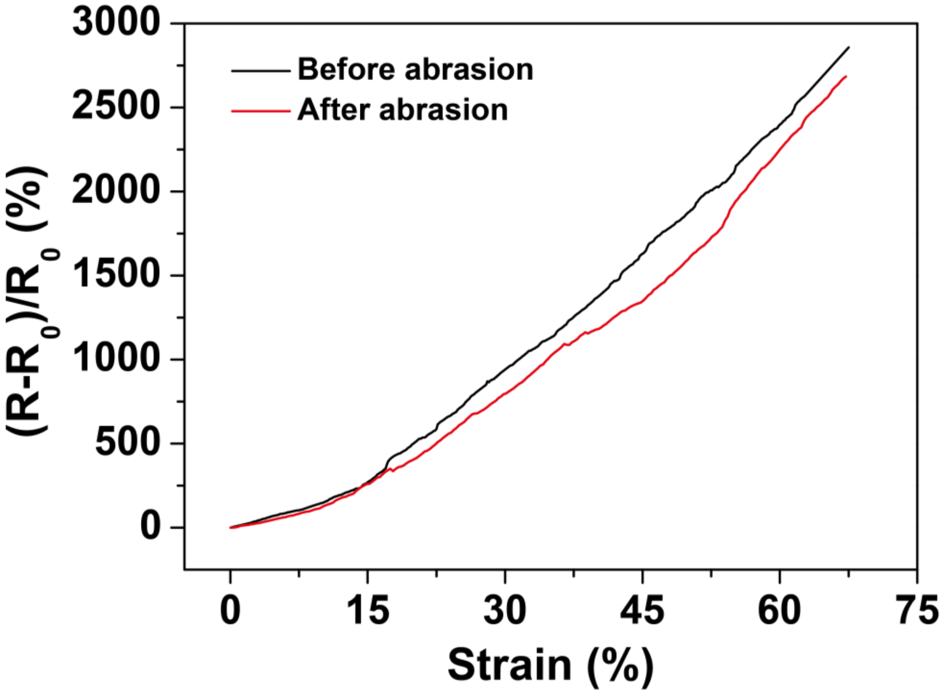

Figure S12. The performance of PPTS-3 before and after abrasion.

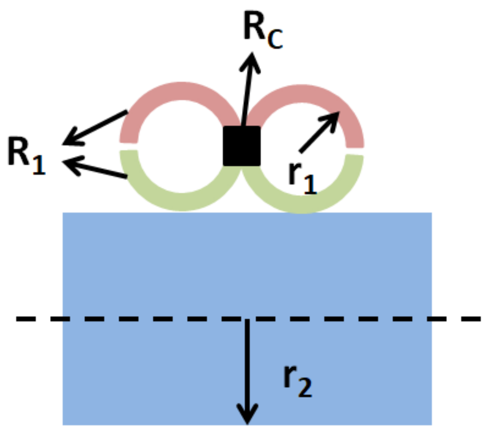

Figure S13. The longitudinal section of the structure.

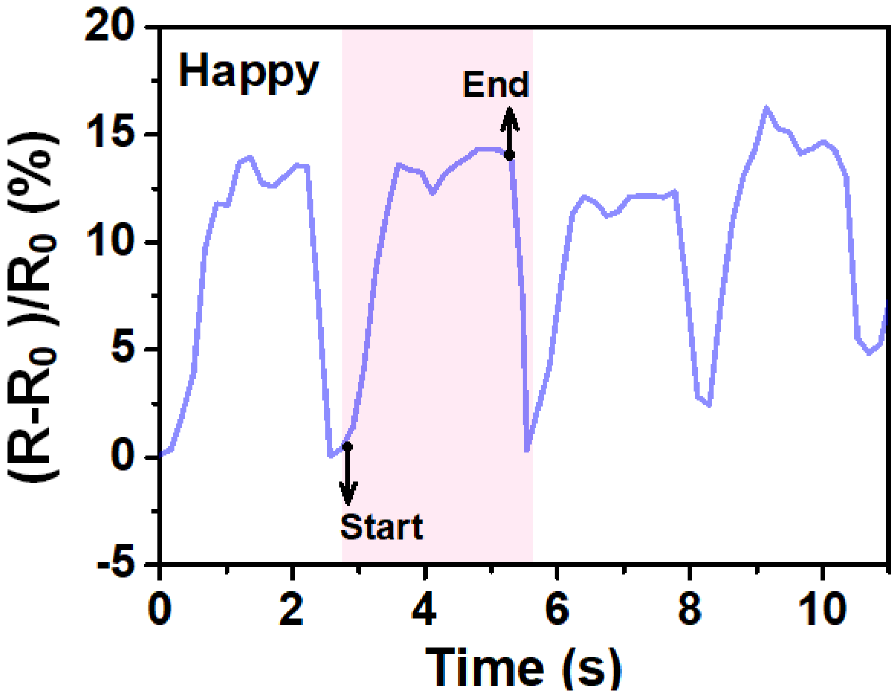

Figure S14. Application of PPTS-M3 for detecting the motion of mouth when the person is happy.

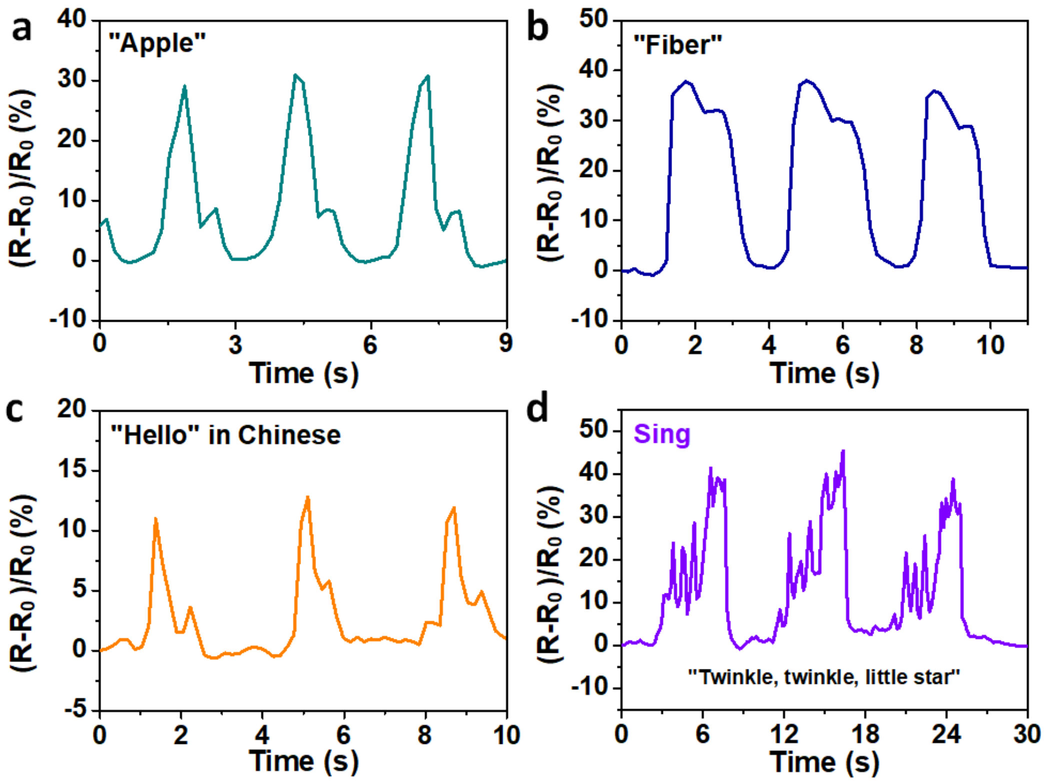

Figure S15. a-b) Applications of PPTS-M3 for vocal cords vibration when speaking “Apple” and “Fiber” in English, respectively. c) Signals when speaking “Hello” in Chinese. d) Signals when singing a song.

Table S1. Performance comparison between our sensors and those reported in literatures.

Strain sensors	Maximal workable strain range	Average gauge factor	Relationship in resistance under strain	Sign of gradient	Ref.
PPy-coated fabrics (Lycra)	60 %	~-3.5 (at 20 % strain) ~-0.7 (at 60 % strain)	None-linear	Negative	1
Graphene based on yarns (NCRY)	150%	1.4	Linear	Positive	2
Graphene based fiber with "compression spring" Structure	100%	10 (1% Strain) 3.7 (50% Strain)	None-linear	Positive	3
Graphene textile without polymer encapsulation	8%	-26	None-linear	Negative	4
Carbonized plain-weave silk fabric with Ecoflex encapsulated	500%	5.8 (under 1% strain) 9.6 (within 250% strain) 37.5 (250%-500% strain)	3 linear regions	Positive	5
Graphene–Nanocellulose Nanopaper	100%	1.6 (10% strain) 7.1 (100% strain)	Exponential	Positive	6
Carbon nanotube film on PDMS	280%	0.82 (40% strain) 0.06 (60-200% strain)	2 linear regions	Positive	7
Carbon black thermal plastic elastomer composite	80%	20	None-linear	Positive	8
Silver nanoparticles	20%	2.05	Linear	Positive	9
Laser-scribed graphene	10%	9.49	Linear	Positive	10
PPTSs	200%	3.8	Linear	Positive	M1
	125%	5.9			M2
	65%	38.9			M3

References

(1). J. Wu, D. Zhou, C. O. Too and G. G. Wallace, *Synth. Met.* **2005**, *155*, 698–701.

(2). J. J. Park, W. J. Hyun, S. C. Mun, Y. T. Park, and O. O. Park, *ACS Appl. Mater. Interfaces* **2015**, *7*, 6317−6324.

(3). Y. Cheng, R. Wang, J. Sun, L. Gao. *Adv. Mater*. **2015**, *27*, 7365.

(4). Z. Yang, Y. Pang, X. L. Han, Y. F. Yang, J. Ling, M. Q. Jian, Y. Y. Zhang, Y. Yang, T. L. Ren, *ACS Nano* **2018**, *12*, 9134-9141.

(5). C. Y. Wang, X. Li, E. L. Gao, M. Q. Jian, K. L. Xia, Q. Wang, Z. P. Xu, T. L. Ren, and Y. Y. Zhang, *Adv. Mater*. **2016**, *28*, 6640–6648.

(6). C. Yan; J. Wang; W. Kang; M. Cui; X. Wang; C. Y. Foo; K. J. Chee; P. S. Lee; *Adv. Mater*. **2014**, *26*, 2022-2027.

(7). T. Yamada, Y. Hayamizu, Y. Yamamoto, Y. Yomogida, A. Izadi-Najafabadi, D. N. Futaba, K. Hata, *Nat. Nanotech*. **2011**, *6*, 296-301.

(8). C. Mattmann, F. Clemens, G. Tröster, *Sensors* **2008**, *8*, 3719-3732.

(9). M. Hempel; D. Nezich; J. Kong; M. Hofmann; *Nano Lett*. **2012**, *12*, 5714–5718.

(10). H. Tian; Y. Shu; Y. L. Cui; W. T. Mi; Y. Yang; D. Xie; T. L. Ren; *Nanoscale* **2014**, *6*, 699–705.